DERIVATIVE DFT BEAMSPACE ESPRIT: A HIGH PERFORMANCE CLOSED-FORM 2-D ARRIVAL ANGLE ESTIMATION ALGORITHM

Cherian P. Mathews

Department of Electrical and Computer Engineering, University of West Florida, Pensacola, FL 32514, USA

ABSTRACT

This paper presents *Derivative DFT Beamspace ESPRIT*, a new closed-form algorithm for direction-of-arrival (DOA) estimation with uniform linear arrays or uniform rectangular arrays. The algorithm uses a novel virtual derivative DFT beamforming procedure to improve upon the performance of the recently developed *DFT Beamspace ESPRIT* algorithm. This beamforming procedure yields an additional invariance relationship which the algorithm exploits to obtain higher estimation accuracy (the algorithm is shown to outperform both *DFT Beamspace ESPRIT* and *Unitary ESPRIT*). Further, Derivative DFT Beamspace ESPRIT possesses all the attractive features (such as low computational complexity, and the ability to provide automatically paired source azimuth and elevation angle estimates) of the two aforementioned algorithms.

1. INTRODUCTION

DFT Beamspace ESPRIT [5, 4]and *Unitary ESPRIT* [5] are recently developed algorithms that provide source DOA estimates via a closed-form procedure when uniform linear linear arrays (ULAs) or uniform rectangular arrays (URAs) are employed. The algorithms when used in conjunction with URAs yield automatically paired source azimuth and elevation angle estimates.

This paper introduces *Derivative DFT Beamspace ESPRIT*, a new closed-form DOA estimation algorithm applicable with ULAs or URAs. This algorithm improves upon *DFT Beamspace ESPRIT* by employing virtual derivative DFT beamforming. Derivative DFT beamforming yields additional invariance relationships which the algorithm incorporates together with with the original set of DFT beamspace relationships. Virtual incorporation of these additional invariances yields improved estimation accuracy without significantly increasing the computational complexity. Results of computer simulations showing that *Derivative DFT Beamspace ESPRIT* can outperform *DFT Beamspace ESPRIT* and *Unitary ESPRIT* are presented.

The work of Anderson [1] provided motivation for employing derivative DFT beamformers to improve estimation accuracy. It was shown in [1] that estimates attaining the element space Cramer-Rao bound could be obtained via reduced dimensional beamspace processing, provided that the column space of the beamformer employed included the array response vectors corresponding to the true arrival directions and their derivatives. *Derivative DFT Beamspace ESPRIT* however operates in a full dimensional beamspace. It employs a full dimensional DFT beamformer and exploits additional invariances that result from a novel virtual derivative beamforming procedure.

Multiple invariances existing in element space with ULAs were exploited by *Multiple Invariance ESPRIT* [3] to improve estimation accuracy. However, this was at the expense of losing the closed-form solution to the DOA estimation problem. This is in contrast with *Derivative DFT Beamspace ESPRIT* which is a closed-form algorithm.

2. DERIVATIVE DFT BEAMSPACE ESPRIT FOR ULAS

We consider an M element ULA with inter-element spacing $\Delta = \lambda/2$, where λ is the wavelength of each of d narrowband plane waves incident on the array. The array output at time t can be modeled as

$$\mathbf{x}(t) = \mathbf{A}\mathbf{s}(t) + \mathbf{n}(t) \tag{1}$$

where $\mathbf{A} = [\mathbf{a}(\mu_1), \cdots, \mathbf{a}(\mu_d)]$ is the DOA matrix, $\mathbf{s}(t)$ is the vector of signal complex envelopes (referenced to the array center), and $\mathbf{n}(t)$ is the vector of noise complex envelopes. The parameter $\mu = 2\pi(\Delta/\lambda)\sin\theta = \pi u$, where $u = \sin\theta$, specifies the source arrival angle; $\theta \in [-\pi/2, \pi/2]$ is the arrival angle measured with respect to the normal to the array axis. The array response vectors are centro-Hermitian due to the choice of the array center as the phase reference, and the corresponding ULA manifold is given by

$$\mathbf{a}(\mu) = e^{-j\frac{M-1}{2}\mu}[1, e^{j\mu}, \ldots, e^{j(M-1)\mu}]^T \tag{2}$$

Derivative DFT beamspace ESPRIT employs the unitary DFT beamforming matrix $\mathbf{W}$ that steers beams in the directions $\mu_m = 2\pi m/M,\ m = 0, 1, \ldots, M-1$. The matrix $\mathbf{W}$ and the corresponding real-valued beamspace manifold $\mathbf{b}(\mu)$ are defined below.

$$\mathbf{W} = \frac{1}{\sqrt{M}}[\mathbf{a}(\mu_0) \vdots \mathbf{a}(\mu_1) \vdots \cdots \vdots \mathbf{a}(\mu_{M-1})] \tag{3}$$

$$\mathbf{b}(\mu) = \mathbf{W}^H\mathbf{a}(\mu) = \frac{1}{\sqrt{M}}[b_0(\mu), b_1(\mu), \ldots, b_{M-1}(\mu)]^T \tag{4}$$

$$\text{where } b_m(\mu) = \mathbf{a}^H(\mu_m)\mathbf{a}(\mu) = \frac{\sin\left[\frac{M}{2}(\mu-\mu_m)\right]}{\sin\left[\frac{1}{2}(\mu-\mu_m)\right]} \tag{5}$$

It was shown in [5] that that the beamspace manifold $\mathbf{b}(\mu)$ satisfies the following invariance property:

$$\tan(\mu/2)\mathbf{\Gamma}_c^M \mathbf{b}(\mu) = \mathbf{\Gamma}_s^M \mathbf{b}(\mu), \text{ where} \tag{6}$$

$$\mathbf{\Gamma}_c^M = \begin{bmatrix} 1 & c_1 & 0 & \cdots & 0 & 0 \\ 0 & c_1 & c_2 & \cdots & 0 & 0 \\ \vdots & \vdots & \vdots & \ddots & \vdots & \vdots \\ 0 & 0 & 0 & \cdots & c_{M-2} & c_{M-1} \\ -1^M & 0 & 0 & \cdots & 0 & c_{M-1} \end{bmatrix} \text{ and}$$

$$\mathbf{\Gamma}_s^M = \begin{bmatrix} 0 & s_1 & 0 & \cdots & 0 & 0 \\ 0 & s_1 & s_2 & \cdots & 0 & 0 \\ \vdots & \vdots & \vdots & \ddots & \vdots & \vdots \\ 0 & 0 & 0 & \cdots & s_{M-2} & s_{M-1} \\ 0 & 0 & 0 & \cdots & 0 & s_{M-1} \end{bmatrix} \tag{7}$$

In the above definitions, $c_i = \cos(\pi i/M)$ and $s_i = \sin(\pi i/M)$. The invariance property (6) was the basis for the development of *DFT Beamspace ESPRIT* [5].

Derivative DFT Beamspace ESPRIT effectively employs derivative DFT beamforming in addition to DFT beamforming. The derivative DFT beamforming weight vector that steers a derivative DFT beam in the direction μ_s is $\dot{\mathbf{a}}(\mu_s)$, where the dot above $\mathbf{a}$ denotes the derivative with respect to μ_s. Eq. 2 yields

$$\dot{\mathbf{a}}(\mu) = \mathbf{D}\mathbf{a}(\mu) \text{ where} \tag{8}$$

$$\mathbf{D} = (j/2)\,\mathrm{diag}\{-(M-1), -(M-3), \cdots, (M-3), (M-1)\}$$

The beamforming matrix that steers derivative DFT beams to the angles $\mu_m = 2\pi m/M$, $m = 0, \ldots, M-1$ is thus $\dot{\mathbf{W}} = \mathbf{D}\mathbf{W}$, where $\mathbf{W}$ is defined in (3). The resulting derivative DFT beamspace manifold, $\mathbf{d}(\mu) = \dot{\mathbf{W}}^H \mathbf{a}(\mu)$, has the form

$$\mathbf{d}(\mu) = \mathbf{W}^H \mathbf{D}^H \mathbf{a}(\mu) = [d_0(\mu), d_1(\mu), \ldots, d_{M-1}(\mu)]^T \tag{9}$$

where $d_m(\mu) = \mathbf{a}^H(\mu_m)\mathbf{D}^H\mathbf{a}(\mu) = -\mathbf{a}^H(\mu_m)\dot{\mathbf{a}}(\mu) = -\frac{d}{d\mu}b_m(\mu)$. Taking the derivative of (5) yields

$$\tan\left(\frac{\mu-\mu_m}{2}\right) d_m(\mu) = \frac{b_m(\mu)}{2} - \frac{M}{2}\frac{\cos\left[\frac{M}{2}(\mu-\mu_m)\right]}{\cos\left[\frac{1}{2}(\mu-\mu_m)\right]}$$

This equation was used in [2] to derive an invariance relationship between adjacent DFT beams and derivative DFT beams. This relationship has the vector form:

$$\tan\left(\frac{\mu}{2}\right)\left[\mathbf{\Gamma}_c^M \mathbf{d}(\mu) - \frac{\mathbf{\Gamma}_s^M}{2}\mathbf{b}(\mu)\right] = \mathbf{\Gamma}_s^M \mathbf{d}(\mu) + \frac{\mathbf{\Gamma}_c^M}{2}\mathbf{b}(\mu) \tag{10}$$

Using (9) and the fact that $\mathbf{W}$ is unitary, we obtain $\mathbf{d}(\mu) = \mathbf{W}^H\mathbf{D}^H(\mathbf{W}\mathbf{W}^H)\mathbf{a}(\mu) = \mathbf{W}^H\mathbf{D}^H\mathbf{W}\mathbf{b}(\mu)$. The DFT beamspace manifold and the derivative DFT beamspace manifold are thus related as follows: $\mathbf{d}(\mu) = \mathbf{F}\mathbf{b}(\mu)$, where $\mathbf{F} = \mathbf{W}^H\mathbf{D}^H\mathbf{W}$. Eq. (10) can now be expressed in terms of just the DFT beamspace manifold. We have

$$\tan(\mu/2)\left[\mathbf{\Gamma}_c^M\mathbf{F} - \frac{\mathbf{\Gamma}_s^M}{2}\right]\mathbf{b}(\mu) = \left[\mathbf{\Gamma}_s^M\mathbf{F} + \frac{\mathbf{\Gamma}_c^M}{2}\right]\mathbf{b}(\mu) \tag{11}$$

The above invariance property, similar in form to (6) that results from DFT beamforming, is formulated entirely in terms of the DFT beamspace manifold $\mathbf{b}(\mu)$. This allows for incorporation of the derivative DFT beamspace invariance relationships in virtual fashion, as described below.

De-emphasizing (11) by a factor k, $0 < k < 1$, (for reasons explained at the end of this section) and adding to (6) yields the following new invariance property that applies to the DFT beamspace manifold $\mathbf{b}(\mu)$:

$$\tan(\mu/2)\,\mathbf{\Gamma}_1^M \mathbf{b}(\mu) = \mathbf{\Gamma}_2^M \mathbf{b}(\mu) \text{ where} \tag{12}$$

$$\begin{aligned} \mathbf{\Gamma}_1^M &= \mathbf{\Gamma}_c^M + k(\mathbf{\Gamma}_c^M\mathbf{F} - \mathbf{\Gamma}_s^M/2) \\ \mathbf{\Gamma}_2^M &= \mathbf{\Gamma}_s^M + k(\mathbf{\Gamma}_s^M\mathbf{F} + \mathbf{\Gamma}_c^M/2) \end{aligned} \tag{13}$$

When d sources impinge on the array, the corresponding *real-valued* beamspace DOA matrix is $\mathbf{B} = \mathbf{W}^H\mathbf{A} = [\mathbf{b}(\mu_1), \cdots, \mathbf{b}(\mu_d)]$. (12) applies to each column of $\mathbf{B}$ and we thus have

$$\begin{aligned} \mathbf{\Gamma}_1^M\mathbf{B}\mathbf{\Omega}_\mu &= \mathbf{\Gamma}_2^M\mathbf{B}, \text{ where} \\ \mathbf{\Omega}_\mu &= \mathrm{diag}\{\tan(\mu_1/2), \cdots, \tan(\mu_d/2)\} \end{aligned} \tag{14}$$

A signal subspace matrix $\mathbf{S} \in \Re^{M\times d}$ that spans the column space of $\mathbf{B}$ can be obtained from the array data (via a singular value decomposition of the beamspace data matrix or an eigenvalue decompositon of the beamspace covariance matrix). We have $\mathbf{B} = \mathbf{S}\mathbf{T}$, where $\mathbf{T}$ is real-valued and non-singular. Writing (14) in terms of $\mathbf{S}$ yields

$$\begin{aligned} \mathbf{\Gamma}_1^M\mathbf{S}\mathbf{\Psi}_\mu &= \mathbf{\Gamma}_2^M\mathbf{S}, \text{ where} \\ \mathbf{\Psi}_\mu &= \mathbf{T}^{-1}\mathbf{\Omega}_\mu\mathbf{T}. \end{aligned} \tag{15}$$

(15) is a real-valued, overdetermined set of equations which can be solved for $\mathbf{\Psi}_\mu$. The eigenvalues of $\mathbf{\Psi}_\mu$ are $\omega_i = \tan(\mu_i/2)$, $i = 1, \ldots, d$. These eigenvalues yield the source DOA estimates: we have $u_i = \sin(\theta_i) = (2/\pi)\tan^{-1}(\omega_i)$.

The de-emphasis factor k in (12) is introduced because derivative DFT beamformers produce higher beamspace noise power than DFT beamformers. Let us assume that the noise vector $\mathbf{n}$ of (1) has covariance matrix $\sigma^2\mathbf{I}$. The DFT beamformer $\mathbf{W}^H$ induces the beamspace noise vector $\mathbf{n}_1 = \mathbf{W}^H\mathbf{n}$ whose covariance matrix is $\sigma^2\mathbf{I}$. The derivative DFT beamformer $\mathbf{W}^H\mathbf{D}^H$ induces the beamspace noise vector $\mathbf{n}_2 = \mathbf{W}^H\mathbf{D}^H\mathbf{n}$, whose covariance matrix is $\sigma^2\mathbf{W}^H\mathbf{D}^H\mathbf{D}\mathbf{W}$. The variance of each element of $\mathbf{n}_2$ is easily shown to be $\sigma^2\mathrm{Tr}\,(\mathbf{D}^H\mathbf{D})/M$. The derivative DFT beamformer thus increases the beamspace noise power by the factor $\mathrm{Tr}\,(\mathbf{D}^H\mathbf{D})/M$. An appropriate deemphasis factor for the derivative DFT beamspace relationships is the reciprocal of the increase in standard deviation. The corresponding value of k is

$$k = \sqrt{\frac{M}{\mathrm{Tr}\,(\mathbf{D}^H\mathbf{D})}} \tag{16}$$

Algorithm Implementation

The first stage of the algorithm is the estimation of the beamspace signal subspace (spanned by the matrix $\mathbf{S}$ of Eq. 15) that is induced by the DFT beamfomer $\mathbf{W}^H$. This

is done by first estimating the signal subspace matrix $\mathbf{S}'$ induced by the beamforming matrix $\mathbf{Q}^H \in \mathcal{C}^{M\times M}$ employed by *Unitary ESPRIT* [5]. The beamformers $\mathbf{W}^H$ and $\mathbf{Q}^H$ are unitary; the signal subspace matrix induced by the DFT beamformer is thus $\mathbf{S} = \mathbf{W}^H\mathbf{Q}\mathbf{S}'$. The following is a summary of *Derivative DFT Beamspace ESPRIT*:

1. Obtain the beamspace data matrix $\mathbf{Y} = \mathbf{Q}^H\mathbf{X}$, where $\mathbf{X} = [\mathbf{x}(1), \mathbf{x}(2), \ldots, \mathbf{x}(K)]$ contains K snapshots of array data. Due to the simple structure of $\mathbf{Q}$, this computation requires only real additions and no multiplications. Form the matrix $\hat{\mathbf{S}}'$ whose columns are the d "largest" left singular vectors of the real-valued matrix $[\mathrm{Re}\{\mathbf{Y}\}, \mathrm{Im}\{\mathbf{Y}\}]$ (see [5]). The size of this real-valued matrix is double that of the original data matrix. This "snapshot doubling" also occurs in element space if forward-backward averaging of data is performed.

2. Compute $\hat{\mathbf{S}} = (\mathbf{W}^H\mathbf{Q})\hat{\mathbf{S}}'$, where $\hat{\mathbf{S}}$ is the signal subspace matrix corresponding to the DFT beamformer $\mathbf{W}^H$. Obtain the least squares (or total least squares) solution $\hat{\mathbf{\Psi}}_\mu$ to the real-valued system of equations $\mathbf{\Gamma}_1^M\hat{\mathbf{S}}\hat{\mathbf{\Psi}}_\mu = \mathbf{\Gamma}_2^M\hat{\mathbf{S}}$. $\mathbf{\Gamma}_1^M$ and $\mathbf{\Gamma}_2^M$ are defined in (13) and k is specified by (16).

3. Compute the eigenvalues $\hat{\omega}_i$, $i = 1, \ldots, d$ of $\hat{\mathbf{\Psi}}_\mu$. The source DOAs are $\hat{u}_i = \sin(\hat{\theta}_i) = (2/\pi)\tan^{-1}(\hat{\omega}_i)$.

The above summary reveals that *Derivative DFT Beamspace ESPRIT* retains all the positive characteristics of *Unitary ESPRIT*; it requires only real-valued computations throughout, incorporates a forward-backward average, and provides a reliability measure (DOA estimates are unreliable if any eigenvalue ω_i in Step 3 is complex-valued). *Derivative DFT Beamspace ESPRIT* requires one more matrix multiplication than *Unitary ESPRIT*. Computing $\hat{\mathbf{S}} = (\mathbf{W}^H\mathbf{Q})\hat{\mathbf{S}}'$ is the additional *real-valued* matrix multiplication required ($\mathbf{W}^H\mathbf{Q}$ is a real-valued matrix that can be precomputed). This is not a significant increase in computational complexity, especially if the number of sources d is small relative to the number of array elements. The simulations of Sec. 4. show that this modest increase in computational complexity is offset by improved estimator performance.

3. DERIVATIVE DFT BEAMSPACE ESPRIT FOR URAS

We consider a $M \times N$ element uniform rectangular array (URA) centered at the origin and lying in the $x-y$ plane. To simplify the development we assume that the inter-element spacing along the x and y directions is $\lambda/2$. In addition to the parameter $\mu = \pi u$, we define $\nu = \pi v$, where $u = \sin\theta\cos\phi$ and $v = \sin\theta\sin\phi$ ($\theta \in [0, \pi/2]$ is the source elevation angle measured down from the z axis, and $\phi \in [0, 2\pi]$ is the source azimuth angle). The array response to a source arriving from the direction (μ, ν) is given by the matrix

$$\mathcal{A}(\mu, \nu) = \mathbf{a}_M(\mu)\mathbf{a}_N^T(\nu) \tag{17}$$

where the subscripts M and N define the size of the vector $\mathbf{a}$ of (2). This response matrix can be vectorized using the *vec* (column stacking) operator. The resulting array manifold is $\mathbf{a}(\mu, \nu) = vec[\mathcal{A}(\mu, \nu)]$.

2-D Derivative DFT Beamspace ESPRIT employs a 2-D DFT beamformer; the corresponding beamspace array response matrix is $\mathcal{B}(\mu, \nu) = \mathbf{W}_M^H\mathbf{a}_M(\mu)\mathbf{a}_N^T(\nu)\mathbf{W}_N^*$, where the subscripts M and N give the dimension of the matrix $\mathbf{W}$ of (3), and the superscript * denotes conjugation. Clearly,

$$\mathcal{B}(\mu, \nu) = \mathbf{b}_M(\mu)\mathbf{b}_N^T(\nu) \tag{18}$$

where $\mathbf{b}(\mu)$ is given by (4). Since $\mathbf{b}_M(\mu)$ satisfies the invariance realtionship (12), we have $\tan(\mu/2)\mathbf{\Gamma}_1^M\mathcal{B}(\mu, \nu) = \mathbf{\Gamma}_2^M\mathcal{B}(\mu, \nu)$ Applying the property $vec(\mathbf{ABC}) = (\mathbf{C}^T \otimes \mathbf{A})vec(\mathbf{B})$, where $\otimes$ denotes the Kronecker matrix product, we find that the stacked beamspace manifold vector $\mathbf{b}(\mu, \nu) = vec[\mathcal{B}(\mu, \nu)]$ satisfies

$$\tan(\mu/2)\mathbf{\Gamma}_{\mu 1}\mathbf{b}(\mu, \nu) = \mathbf{\Gamma}_{\mu 2}\mathbf{b}(\mu, \nu) \quad \text{where} \tag{19}$$

$$\mathbf{\Gamma}_{\mu 1} = \mathbf{I}_N \otimes \mathbf{\Gamma}_1^M \quad \text{and } \mathbf{\Gamma}_{\mu 2} = \mathbf{I}_N \otimes \mathbf{\Gamma}_2^M \tag{20}$$

Now, the 1-D beamspace manifold $\mathbf{b}_N(\nu)$ satisfies the invariance property $\tan(\nu/2)\mathbf{\Gamma}_1^N\mathbf{b}_N(\nu) = \mathbf{\Gamma}_2^N\mathbf{b}_N(\nu)$. Using this in (18) yields $\tan(\nu/2)\mathcal{B}(\mu, \nu)(\mathbf{\Gamma}_1^N)^T = \mathcal{B}(\mu, \nu)(\mathbf{\Gamma}_2^N)^T$. Applying the stacking property now yields

$$\tan(\nu/2)\mathbf{\Gamma}_{\nu 1}\mathbf{b}(\mu, \nu) = \mathbf{\Gamma}_{\nu 2}\mathbf{b}(\mu, \nu) \quad \text{where} \tag{21}$$

$$\mathbf{\Gamma}_{\nu 1} = \mathbf{\Gamma}_1^N \otimes \mathbf{I}_M \quad \text{and } \mathbf{\Gamma}_{\nu 2} = \mathbf{\Gamma}_2^N \otimes \mathbf{I}_M \tag{22}$$

Applying (19) to the $MN \times d$ dimensional beamspace DOA matrix $\mathbf{B} = [\mathbf{b}(\mu_1, \nu_1), \ldots, \mathbf{b}(\mu_d, \nu_d)]$ yields

$$\begin{aligned} \mathbf{\Gamma}_{\mu 1}\mathbf{B}\mathbf{\Omega}_\mu &= \mathbf{\Gamma}_{\mu 2}\mathbf{B}, \text{ where} \\ \mathbf{\Omega}_\mu &= \mathrm{diag}\{\tan(\mu_1/2), \cdots, \tan(\mu_d/2)\} \end{aligned} \tag{23}$$

Similarly, applying (21) to the DOA matrix $\mathbf{B}(\mu, \nu)$ yields

$$\begin{aligned} \mathbf{\Gamma}_{\nu 1}\mathbf{B}\mathbf{\Omega}_\nu &= \mathbf{\Gamma}_{\nu 2}\mathbf{B}, \text{ where} \\ \mathbf{\Omega}_\mu &= \mathrm{diag}\{\tan(\nu_1/2), \cdots, \tan(\nu_d/2)\} \end{aligned} \tag{24}$$

The signal subspace matrix $\mathbf{S}$ that spans the column space of $\mathbf{B}$ can be obtained as follows. Let K snapshots of array data (in vectorized form) be grouped to form the $MN \times K$ data matrix $\mathbf{X}$. The corresponding (vectorized) DFT beamspace data matrix is $\mathbf{Y} = (\mathbf{W}_N^H \otimes \mathbf{W}_M^H)\mathbf{X}$ [5]. The d signal eigenvectors that comprise the columns of $\mathbf{S}$ are the d "largest" left singular vectors of the real-valued matrix $[\mathrm{Re}\{\mathbf{Y}\}, \mathrm{Im}\{\mathbf{Y}\}]$. We have $\mathbf{S} = \mathbf{BT}$ where $\mathbf{T}$ is a non-singular *real-valued* matrix. Substituting $\mathbf{B} = \mathbf{S}\mathbf{T}^{-1}$ in (23) and (24) yield the signal eigenvector relationships

$$\begin{aligned} \mathbf{\Gamma}_{\mu 1}\mathbf{S}\mathbf{\Psi}_\mu = \mathbf{\Gamma}_{\mu 2}\mathbf{S} \quad &\text{where} \quad \mathbf{\Psi}_\mu = \mathbf{T}^{-1}\mathbf{\Omega}_\mu\mathbf{T} \\ \mathbf{\Gamma}_{\nu 1}\mathbf{S}\mathbf{\Psi}_\nu = \mathbf{\Gamma}_{\nu 2}\mathbf{S} \quad &\text{where} \quad \mathbf{\Psi}_\nu = \mathbf{T}^{-1}\mathbf{\Omega}_\nu\mathbf{T} \end{aligned} \tag{25}$$

All the quantities in the above expressions for $\mathbf{\Psi}_\mu$ and $\mathbf{\Psi}_\nu$ are real-valued. We thus have $\mathbf{\Psi}_\mu + j\mathbf{\Psi}_\nu = \mathbf{T}^{-1}(\mathbf{\Omega}_\mu + j\mathbf{\Omega}_\nu)\mathbf{T}$. The eigenvalues of the complex-valued matrix $\mathbf{\Psi}_\mu + j\mathbf{\Psi}_\nu$ are thus $\omega_i = \tan(\mu_i/2) + j\tan(\nu_i/2)$, $i = 1, \ldots, d$. These eigenvalues provide properly paired arrival angle estimates for each source. The direction cosines of the ith source relative to the x and y axes are $u_i = (2/\pi)\tan^{-1}[\mathrm{Re}(\omega_i)]$ and $v_i = (2/\pi)\tan^{-1}[\mathrm{Im}(\omega_i)]$,

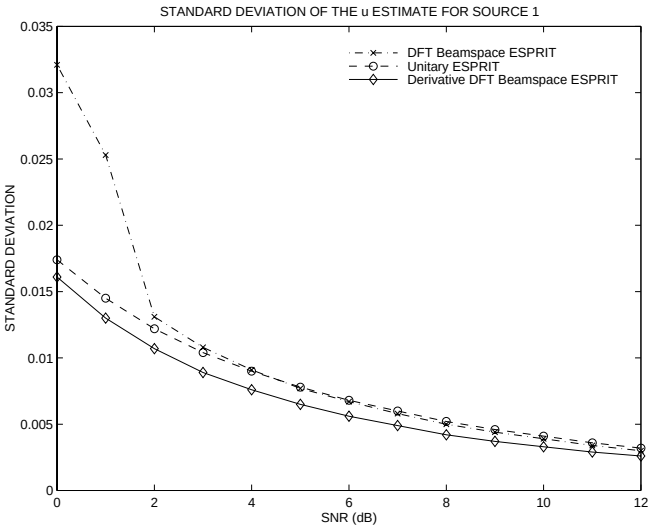

Figure 1: Algorithm performance for a 10 element ULA: Statistics for source 1.

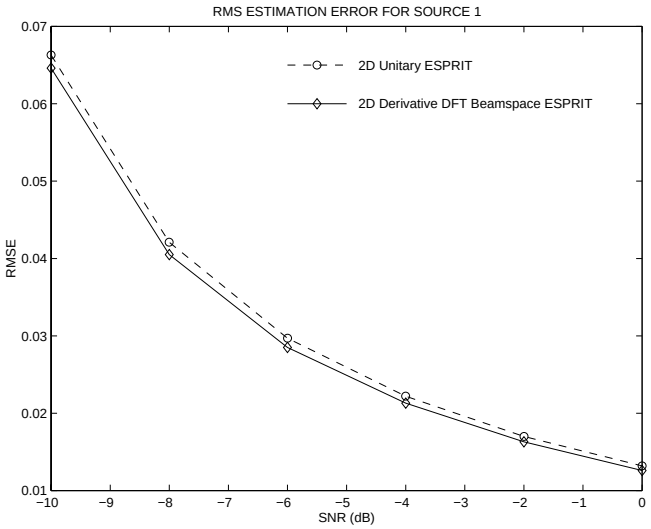

Figure 2: Algorithm performance for a 4×4 URA: Statistics for source 1.

respectively. The implementation of *2-D Derivative DFT Beamspace ESPRIT* is similar to that outlined earlier for the 1-D case. The appropriate value for the de-emphasis factor k for the 2-D case can be shown to be $k = \sqrt{MN}/\sqrt{\mathrm{Tr}(\mathbf{D}_M^H\mathbf{D}_M)\mathrm{Tr}(\mathbf{D}_N^H\mathbf{D}_N)}$, where $\mathbf{D}_M$ was defined in (8).

4. RESULTS OF COMPUTER SIMULATIONS

Computer simulations were performed using a 10 element ULA with inter-element spacing $\Delta = \lambda/2$. The source scenario consisted of two equipowered, uncorrelated sources located at $\theta = -3^\circ$ and 3° (source separation $\approx 26\%$ of the mainlobe width). The relative performance of *DFT Beamspace ESPRIT*, *Derivative DFT Beamspace ESPRIT*, and *Unitary ESPRIT* as a function of the common source SNR was investigated. Sample estimator statistics were obtained using 800 independent trials and K=64 data snapshots per trial. Fig. 1 depicts the sample standard deviation of the u estimate of the first source (performance curves for the second source are not depicted because they are similar to those of the first). The figure shows that *Derivative DFT Beamspace ESPRIT* outperforms *Unitary ESPRIT*. The standard deviation of the *Derivative DFT Beamspace ESPRIT* estimates for source 1 is an average of 16% lower than that of the *Unitary ESPRIT* estimates over the SNR range 0 to 12dB. It is also evident from the figure that *Derivative DFT Beamspace ESPRIT* outperforms (full dimensional) *DFT Beamspace ESPRIT*.

Simulations for the 2D versions of the algorithms were performed using a 4×4 uniform rectangular array with half-wavelength interelement spacings along the x and y directions. The simulation included two equipowered, uncorrelated sources located at $(u_1, v_1) = (-0.125, -0.125)$ and $(u_2, v_2) = (0.125, 0.125)$. 800 independent trials were conducted with 64 snapshots per trial. Fig. 2 depicts the rms estimation error for the first source, as a function of the common source SNR (The rms error for source i is $RMSE_i = \sqrt{E\{(\hat{u}_i - u_i)^2\} + E\{(\hat{v}_i - v_i)^2\}}$). The figure reveals that *2D Derivative DFT Beamspace ESPRIT* performs better than *2D Unitary ESPRIT*.

5. CONCLUSIONS

Derivative DFT Beamspace ESPRIT, a new closed-form algorithm for DOA estimation with ULAs and URAs has been presented. The 2-D version of the algorithm provides automatically paired source azimuth and elevation angle estimates via a closed-form procedure (computationally expensive search procedures are not required). The algorithm exploits invariance relationships resulting from derivative DFT beamforming in a novel virtual fashion to improve estimation accuracy. The estimator performance is shown to be superior to that of *DFT Beamspace ESPRIT* and *Unitary ESPRIT*.

REFERENCES

[1] S. Anderson. On optimal dimension reduction for sensor array signal processing. *Signal Processing*, 30(2):245–256, January 1993.

[2] C.P. Mathews. Improved closed-form DOA/frequency estimation via ESPRIT using DFT and derivative DFT beamforming. In *Proc. IEEE Int. Conf. Acoust., Speech, Signal Processing*, pages 2916–2919, vol. 5, 1996.

[3] A. Swindlehurst, B. Ottersten, R. Roy, and T. Kailath. Multiple invariance ESPRIT. *IEEE Trans. on Signal Processing*, 40(4):867–881, April 1992.

[4] M.D. Zoltowski, M. Haardt, and C.P. Mathews. Closed-form 2D angle estimation with rectangular arrays via DFT Beamspace ESPRIT. In *28th Asilomar IEEE Conference on Signals, Systems, and Computers*, pages 682–686, 1994.

[5] M.D. Zoltowski, M. Haardt, and C.P. Mathews. Closed-form 2D angle estimation with rectangular arrays in element space or beamspace via Unitary ESPRIT. *IEEE Trans. on Signal Processing*, pages 316–328, February 1996.